MedChemComm

RESEARCH ARTICLE

View Article Online
View Journal

Cite this: DOI: 10.1039/c6md00262e

Biophysical investigation and conformational analysis of p38α kinase inhibitor doramapimod and its analogues†‡

Amir H. Nasiri,[a] Krishna Saxena,[ab] Jan W. Bats,[a] Hamid R. Nasiri*[a] and Harald Schwalbe*[ab]

Received 12th May 2016,
Accepted 23rd May 2016

DOI: 10.1039/c6md00262e

www.rsc.org/medchemcomm

Doramapimod (BIRB 796) is a potent inhibitor of p38α mitogen-activated protein kinase. It contains an aryl-pyrazole scaffold as a pharmacophore critical for binding. The aryl-pyrazole scaffold is not planar and adopts an out-of-plane conformation, which is described by the torsion angle θ. In this letter, we report the chemical synthesis and biophysical characterization of different analogues of doramapimod (**3–12**) exhibiting distinctly different aryl-pyrazole torsion angle θ values. The torsion angle θ values of the synthesized analogues (**3–6**) were determined by crystal structural analysis and the binding affinities to p38α kinase investigated by microscale thermophoresis. Our results unveil a clear correlation between kinase binding and the torsion angle θ of tested doramapimod analogues, highlighting the importance of inhibitor conformation for protein binding.

Introduction

p38α mitogen-activated protein (MAP) kinase is involved in stimulated inflammation[1] and plays an important role in the MAP kinase signalling pathway. The vital regulatory behaviour of protein kinases, their involvement in different biological pathways and their druggable properties promote them as major drug targets of the twenty-first century.[2] Inhibition of protein kinases by small molecules appears to be an attractive therapeutic approach for the treatment of cancer and autoimmune diseases.[3] There are more than 518 putative protein kinase genes identified in the human genome[4] and many kinase inhibitors are currently in clinical development or already on the market.[5] Doramapimod (BIRB 796; 1-(5-*tert*-butyl-2-*p*-tolyl-2*H*-pyrazol-3-yl)-3-[4-(2-morpholin-4-yl-ethoxy)-naphthalen-1-yl]-urea) (**1**) (Fig. 1) is a potent type II inhibitor of p38α kinase with a K_d of 0.1 nM.[6] It was developed by Boehringer Ingelheim Pharmaceuticals, starting from fragment **2**,[6] in a hit-to-lead program.[7] Doramapimod made it to late-stage clinical trial for treatment of rheumatoid arthritis and Crohn's disease. Doramapimod utilizes a second binding pocket spatially distinct from the ATP-binding site. The co-crystal structure of the inhibitor **3**, an analogue of doramapimod (**1**), bound to human p38α kinase revealed that the binding is predominately defined by hydrogen bonding and hydrophobic interactions (Fig. 1).[7] Similar to doramapimod (**1**), compound **3** binds to a conserved region of protein kinases, the so-called DFG-loop (p38α kinase: Asp(D)168-Phe(F)169-Gly(G)170) and stabilizes this loop in a single conformation, also known as DFG-out conformation. Inhibitors that preferably bind to the DFG-out conformation are called "type II" inhibitors in contrast to the "type I" inhibitors that bind to the DFG-in conformation. It has been postulated that kinase inhibitors, which bind and stabilize the DFG-out conformation, provide a better starting point for follow-up optimization compared to their counterparts that bind and stabilize p38α kinase in the active DFG-in conformation. However, a recent study on type II inhibitors unveiled that type II inhibitors may not be *per se* more selective than type I inhibitors.[8]

In the co-crystal structure, the phenyl part of inhibitor **3** is buried deeply in a hydrophobic pocket forming additional interaction to Glu71 *via* a π-CH_2 lipophilic contact.[7,9]

Based on the interaction between the inhibitor **3** and the human p38α kinase, Regan and co-workers highlighted the importance of torsion angle θ in the aryl-pyrazole core for binding affinity.[7] Based on their hypothesis, for an optimal lipophilic interaction, the torsion angle θ should be around 54°; and this conformation was referred to as bioactive conformation. The twist angle θ of doramapimod is below this value (46.5°).[6] The loss of binding affinity of compound **5**,

[a] *Institute of Organic Chemistry and Chemical Biology, Center for Biomolecular Magnetic Resonance (BMRZ), Johann Wolfgang Goethe-University Frankfurt, Max-von-Laue-Straße 7, D-60438 Frankfurt am Main, Germany.*
E-mail: schwalbe@nmr.uni-frankfurt.de, Nasiri@nmr.uni-frankfurt.de
[b] *German Cancer Consortium (DKTK), German Cancer Research Center (DKFZ), Heidelberg, Germany*

† The authors declare no competing interests.

‡ CCDC 1474053–1474059. For crystallographic data in CIF or other electronic format see DOI: 10.1039/c6md00262e

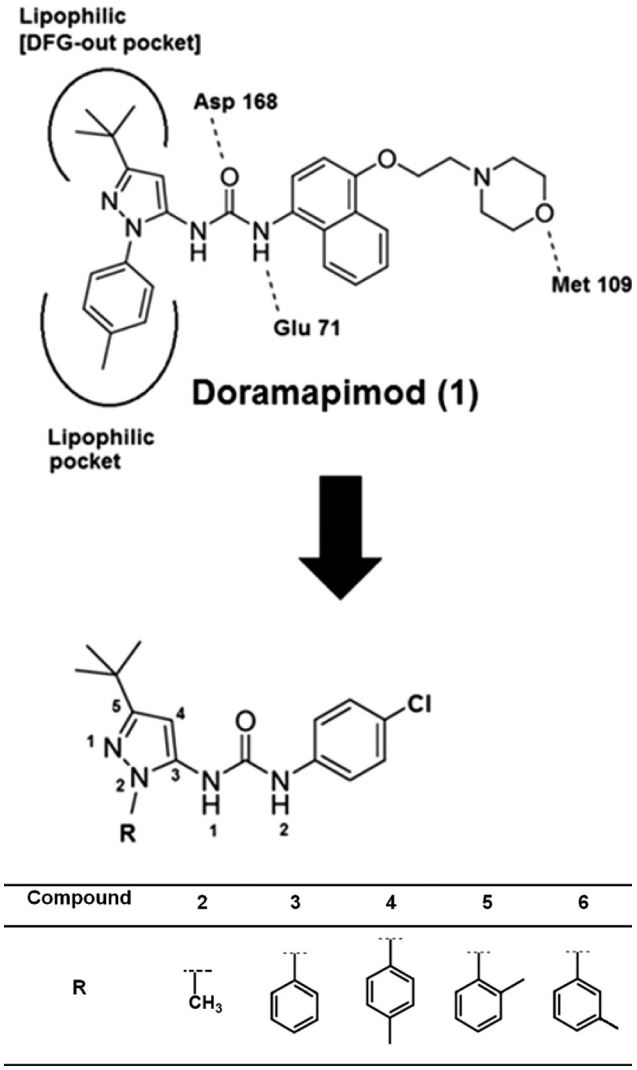

Fig. 1 Key interactions of doramapimod (**1**) with p38α kinase according to Regan and co-workers[6] (PDB code 1KV2). Constitution of fragment **2** and doramapimod analogues **3**–**6** investigated in this study.

with a substituent in the *ortho*-position was explained by a possible increase of the torsion angle θ beyond the favoured 54° (Fig. 1).

To test this hypothesis of an inhibitor bioactive conformation and to investigate the influence of the torsion angle on binding affinity, a conformational analysis was carried out with the main focus on the torsion angle θ. This analysis was conducted by the chemical modification of doramapimod (**1**) within the aryl-pyrazole region (Fig. 1). Doramapimod (**1**) has been subjected to different structure–activity relationship (SAR) studies focussing on the urea-,[7] the morpholine part,[9] ethoxy morpholino-[10] and ethoxy naphthalene modification.[11] For the modification of the aryl-pyrazole part, derivatives of doramapimod (**3**–**12**) were synthesized. The DFG-out mode of binding of this class of molecules was confirmed by using nuclear magnetic resonance (NMR) spectroscopy. The torsion angle θ of the analogues (**3**–**6**) were characterized by small-molecule X-ray crystallography. Microscale thermophoresis (MST) was applied to determine the corresponding K_i values against p38α kinase. A clear correlation was found between ligand conformation and kinase binding affinities.

Results and discussion

Compounds **3**–**6** were selected in order to test the influence of aryl-pyrazole ring substituents on the torsion angle θ and p38α kinase binding.

Co-crystal structures of compounds **2** and **3** bound to p38α kinase have been reported by Pargellis[6] and Regan.[7] These structures gave us the opportunity to compare the conformation of the protein-bound ligand with the conformation of the free ligand. Compound **4** represents the original aryl part of doramapimod with a methyl group in the *para*-position.

For compounds similar to **5**, with a methyl group in the *ortho*-position, a decrease in activity was reported.[7] The determination of twist angle θ of both compounds **4** and **5** would be helpful to rationalize the reported differences in activities. All compounds were synthesized by the condensation of the corresponding substituted phenyl-1*H*-pyrazol-5-amines with 4-chlorophenyl isocyanate.[7] The substituted phenyl-1*H*-pyrazol-5-amines were prepared from 4,4-dimethyl-3-oxopentanenitrile and substituted phenyl-hydrazines,[7] known as the Knorr pyrazole synthesis (see Scheme 1). The synthesis of compounds **4**–**6** has been previously reported.[12]

Single crystals of doramapimod analogues **3**–**6** suitable for X-ray crystal structure analysis were obtained from dimethylsulfoxide or methanol solutions. The values of torsion angles θ of synthesized analogues were listed in Fig. 2.

Due to the N1-pyrazole basicity and N–H urea hydrogen-bound donation property, solvated complexes of **3** and **5** were obtained. In solution, there is a free rotation around the pyrazole-aryl planes of these molecules, which makes them quite flexible and allows them to adopt multiple conformations in solution. In solid state, however, analogues **3** and **4** with a similar aryl-pyrazole part present in doramapimod have distinct torsion angles between 34.5° and 47°. Comparison of these values with the bioactive conformation shows only a slight deviation. In contrast, the introduction of the methyl group in *ortho*-position led to an increase of the torsion angle θ (82.2° and 72.8°). These values are beyond the bioactive conformation (θ = 54°) and would explain the loss of activity.

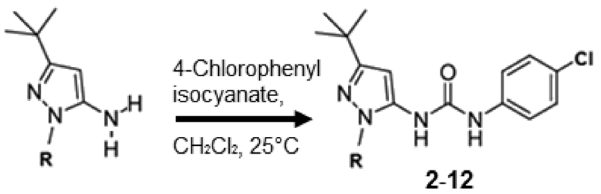

Scheme 1

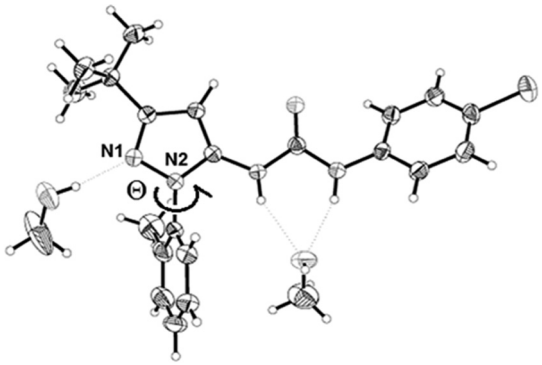

Compound	3	4	5	6
Θ	47.0[a] 34.5[b,+] 40.5 [b,+]	38.1	72.8[a] 82.2[b]	37.3[c]

[a]as methanol complex
[b]as dimethylsulfoxide complex
[+]unit cell contains two crystallographically independent molecules
[c]value calculated from the hydrochloride complex

Fig. 2 Perspective view of the X-ray structure of **5** as a methanol solvated complex, showing the displacement ellipsoids drawn at the 50% probability level with the dihedral angle θ between the pyrazole/σ-tolyl planes (N1–N2–C–C). Dihedral angle values for derivatives **3**–**6**.

To confirm the DFG-out binding mode of these type II compounds 2D-NMR technique was used in combination with selectively ^{15}N-Phe-isotope labelled p38α kinase. The p38α kinase contains 13 phenylalanine residues (see ESI‡), of which 12 can be detected and unambiguously assigned in the ^{1}H–^{15}N TROSY spectrum of the apo-form[13] (Fig. 3). The missing signal belongs to Phe169, which is part of the flexible DFG-loop. As previously reported, the DFG-loop of the p38α kinase apo-form is involved in a DFG-in/DFG-out conformational exchange process on an intermediate timescale, causing a strong line broadening and missing of the Phe169 signal.

Addition of the fragment **2** arrests the DFG-loop of p38α kinase in the DFG-out conformation, resulting in the detection of the missing Phe169 signal in the ^{1}H–^{15}N TROSY spectrum (Fig. 3). Similar results were obtained with the other analogues containing the pyrazole-urea scaffold (see ESI‡).

The binding affinities of synthesized analogues to p38α kinase were investigated by microscale thermophoresis (MST). MST has recently emerged as a powerful technique to investigate ligand-kinase interactions.[14] The affinities for the interaction is quantified by monitoring the directed movement of fluorescent molecules in microscopic temperature gradients.[15] All the tested compounds against p38α kinase revealed accurate MST traces with no sign of protein aggregation or denaturation. As an example the MST thermogram of compound **3** is shown in Fig. 4. All investigated derivatives show similar binding curves.

Compounds were tested against the inactive and active form of the p38α kinase. No differences in inhibition constants were observed, indicating that this type of inhibitors has the same affinity for p38α kinase irrespective of its phosphorylation state: This finding has already been reported for doramapimod[16] and is in line with our previous NMR investigations showing the dynamic status of the DFG-loop in the unphosphorylated and phosphorylated kinase.[17] The inhibition constants for analogues **2**–**6** are summarized in Fig. 4.

The K_i values for compounds **2** and **4**–**6** determined by MST are in good agreement with reported values from binding studies using an acrylodan-fluorescently labelled p38α kinase.[12]

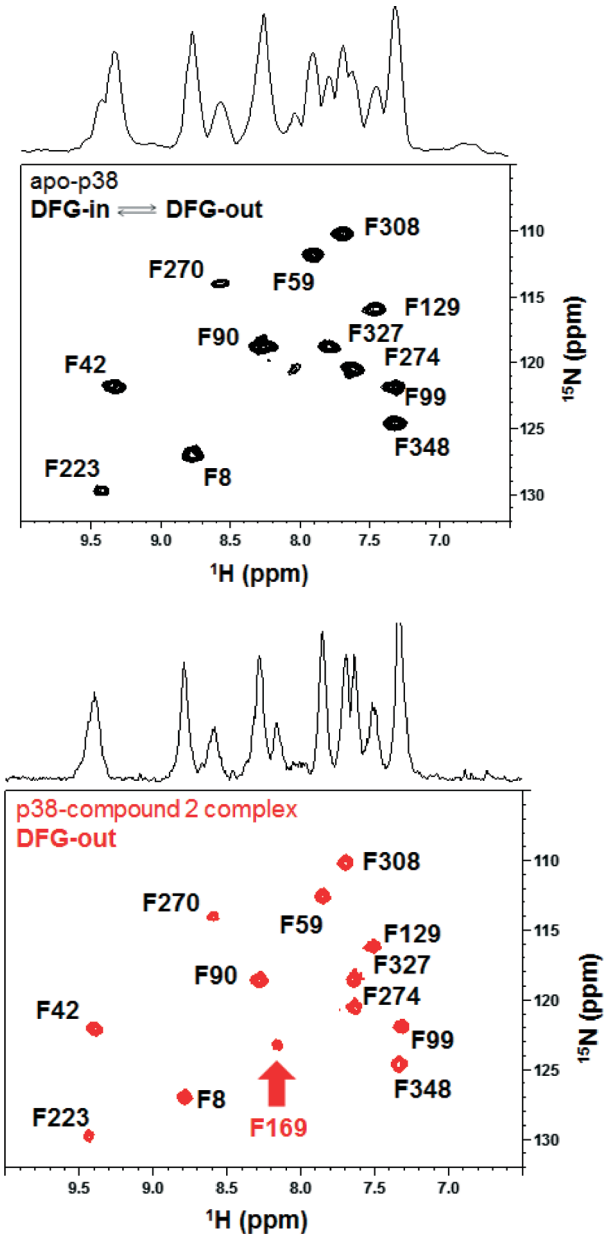

Fig. 3 ^{1}H–^{15}N TROSY spectra of ^{15}N-pheylananine-labeled p38α kinase in the apo-state (in black) and after the addition of fragment **2** (in red). The addition of fragment **2** results in the appearance of a new peak (indicated by an arrow) in the spectrum.

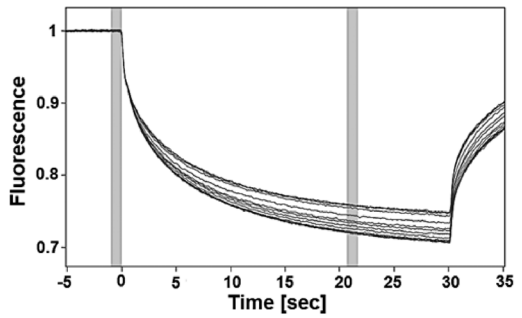

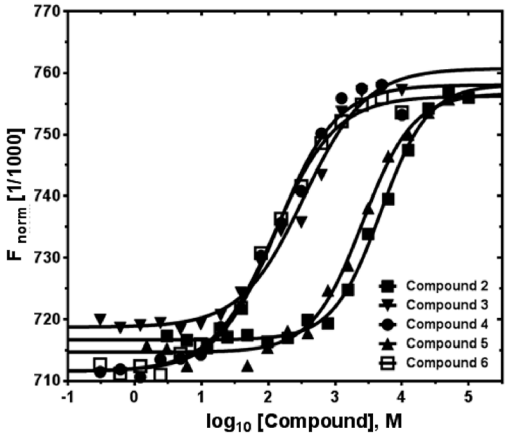

Compound	2	3	4	5	6
K_i [μM]	1.29 ± 0.37	0.10 ± 0.003	0.03 ± 0.01	0.73 ± 0.26	0.02 ± 0.01

Fig. 4 MST measurements for the binding of doramapimod analogues to the inactive p38α kinase. MST thermogram of compound **5** in concentrations ranging from 1.5 nM to 50 μM against a fix concentration of p38α kinase (80 nM) and tracer (25 nM). MST experimental binding curves of derivatives **3**–**6**. Data are expressed as the mean of three independent runs. Data were fitted using a variable slope four parameters fit (R-square >0.98). K_i = inhibition constant, determined by microscale thermophoresis. Data from competition experiment against p38α kinase.

Analogues **4** and **6** are three to fivefold more potent compared to analogue **3**. This is due to the introduction of the methyl group which increases the lipophilicity of these compounds as reflected in their calculated log*P* values (**3** log*P* = 5.6, **4** log*P* = 6.0 and **6** log*P* = 6.2) and hence increases the binding affinity towards the hydrophobic pocket of p38α kinase. In contrast, compound **5**, with similar lipophilicity (log *P* = 6.2) but with an increase torsion angle value (θ = 77.5°) revealed a decrease of affinity by sevenfold compared to compound **3**. The data show a clear correlation between kinase binding affinities and the torsion angle θ of the inhibitors.

To further investigate the influence of ligand conformation on kinase binding, additional compounds (**7**–**12**) were synthesized (Fig. 5).

Pairs of *ortho*- and *para*-substituted doramapimod analogues were selected with respect to the spatial requirements of the substituents. Analogues **7**–**12** were tested against p38α kinase by MST (Fig. 6). As expected, the small fluorine substituent showed no differences in potency when introduced either in the *para*-**7** or *ortho*-position **8**, compared to the unsubstituted compound **3**.

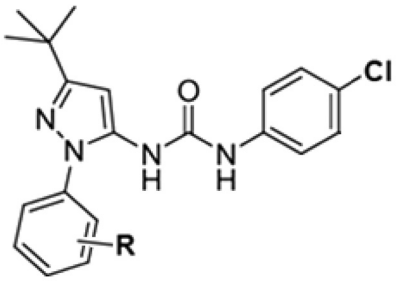

Compound	7	8	9	10	11	12
R	F	F	OCH_3	OCH_3	Cl	Cl
Position	*para*	*ortho*	*para*	*ortho*	*para*	*ortho*

Fig. 5 Constitution of doramapimod analogues **7**–**12**, with different substitutions in the *para*- and *ortho*-position.

In contrast, when larger substituents (*i.e.* chlorine or methoxy-group) were introduced clear differences in inhibition were observed. The *ortho*-substituted analogues (**10** and **12**) were significantly less active compared to their *para*-substituted counterparts (**9** and **11**).

For fragment **2**, compared with doramapimod (**1**) and the analogues **3**–**12**, the *N*-phenyl-1*H*-pyrazole scaffold, and thereby the attractive hydrophobic interaction is missing (log *P* = 4.3). The lack of this hydrophobic interaction is reflected in its low binding affinity (K_i = 1.29 μM), as the K_i increases by thirteen fold compared to compound **3**. This is in agreement with the reported data.[7] Compound **2** also shows different crystallization behaviour. The X-ray structure contains

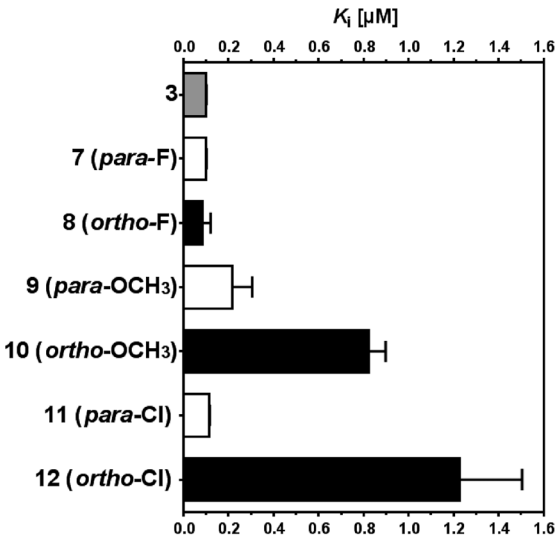

Fig. 6 Inhibition constants of pairs of *ortho*- and *para* substituted analogues. Data were generated from competition experiments against the inactive p38α kinase and expressed as the mean of three independent runs. Compound **3** was used as a control.

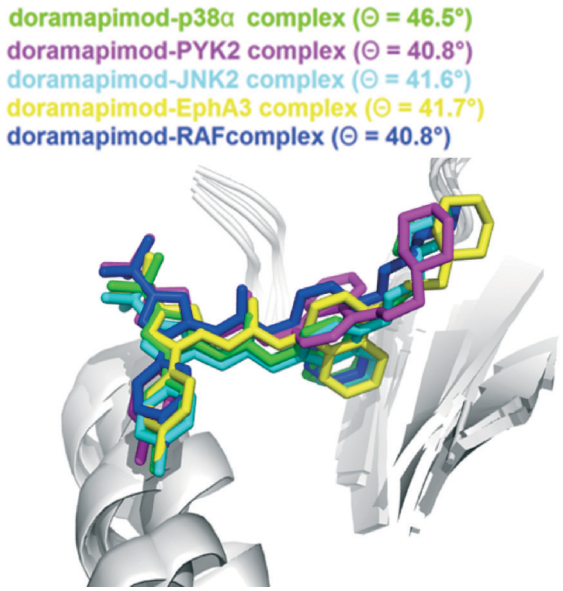

Fig. 7 Superposition of the crystal structures of p38α kinase (PDB code 1KV2), PYK2 (PDB code 3FZS), JNK2 (PDB code 3NPC), EphA3 (PDB code 4TWN) and B-raf (PDB code 4JVG) in complex with doramapimod (**1**). The figure was generated using PyMOL program.[22]

three independent molecules with significantly different conformations. Each molecule contains three planar planes. For the three independent molecules the angles between the pyrazole–urea, urea–phenyl and pyrazole–phenyl are respectively 30.6/86.3/84.5°, 34.3/30.6/10.5° and 9.3/67.5/84.7°. The pyrazole–urea, urea–phenyl and pyrazole–phenyl torsion angles for the protein bound conformation **2** are 41.96/41.86 and 69.27.[6] This finding underscores the highly flexible nature of fragment **2** even in the solid state.

For a rational drug discovery approach, doramapimod was also co-crystalized with c-Jun N-terminal kinase 2 (JNK2) a closely related mitogen-activated protein kinase.[18] Additional structures of doramapimod in complex with RAF kinase,[19] a member of the serine/threonine protein kinase family, as well as with tyrosine kinases PYK2[20] and EphA3[21] were also reported. In all these structures, doramapimod stabilizes the DFG-out conformation of the respective kinases.

A closer look at the dihedral angle θ between the pyrazole/*p*-tolyl planes, reveals that doramapimod adopts the same bioactive conformation with a dihedral angle of $\theta \sim 42.3°$. Our findings of the bioactive conformation of doramapimod, seems to be generalizable to other kinase-doramapimod complexes. The overlay of doramapimod bound to the respective kinases is highlighted in Fig. 7.

Conclusions

In summary, we showed that the structures of doramapimod and analogues are highly flexible in solution, whereas in solid state they adopt a conformation belonging to one of the local energy minima. This conformation differs slightly from the protein-bound conformation. Therefore, the recognition process presumably follows the conformational selection mechanism of ligand binding to p38α kinase.

In general, consideration of ligand conformation is important for a successful ligand based inhibitor design.

The ability of both determining conformational properties of small molecule and their effect on target binding is indispensable for drug discovery as demonstrated for the cannabinoid CB1 receptor antagonists[23] and hepatitis C virus NS5B RNA polymerase inhibitors.[24] In both case studies conformational characteristics of the interaction of the ligand with its respective target were determined. Subsequently, conformational-based restrictions of ligand flexible torsion angles were used to guide the identification of new inhibitors. As a result conformational constrained analogues with increased potencies were identified.[23,24] In this study we have analyzed the conformational properties of doramapimod analogues and revealed a clear correlation between p38α kinase binding and the torsion angle θ. The presented study provides strong support for the incorporation of ligand conformational analysis into the common SAR studies for conformationally flexible ligands.

Experimental part

Chemistry

General remarks. NMR spectra were recorded on Bruker DPX250 and AVII300 spectrometers operating at a ^{1}H frequency of 250 MHz or 300 MHz and at ^{13}C frequency of 62.9 MHz. Elementary analyses were measured on a Foss Heraeus CHN-O-RAPID instrument. All reactions were monitored by thin-layer chromatography (TLC), performed on silica gel POLYgram® (Macherey-Nagel). Chromatographic purifications were done with Merck silica gel 60.

5-*tert*-Butyl-2-(2-fluoro-phenyl)-2*H*-pyrazol-3-yl-amine, 3-*tert*-butyl-1-(4-methoxyphenyl)-1*H*-pyrazol-5-amine and 3-*tert*-butyl-1-(2-methoxyphenyl)-1*H*-pyrazol-5-amine were purchased from Fluorochem. 3-*tert*-butyl-1-(4-fluoro-phenyl)-1*H*-pyrazol-5-amine, 3-*tert*-butyl-1-(2-chloro-phenyl)-1*H*-pyrazol-5-amine, 3-*tert*-butyl-1-(4-chloro-phenyl)-1*H*-pyrazol-5-amine and 4-chlorophenyl isocyanate were purchased from Sigma Aldrich.

1-(5-*tert*-Butyl-2-methyl-2*H*-pyrazol-3-yl)-3-(4-chlorophenyl)-urea (2) and 1-(3-*tert*-butyl-2-methyl-2*H*-pyrazol-5-yl)-3-(4-chlorophenyl)urea (iso-2). A solution of 4,4-dimethyl-3-oxo-pentanenitrile (18 mmol, 2.25 g) and methyl hydrazine (19 mmol, 0.875 g, 1 mL) in toluene (7.5 mL) was heated to reflux overnight. Toluene was removed *in vacuo*. The residue was dissolved in dichloromethane (DCM) and washed with water and brine. After concentration *in vacuo* 2.5 g of crude amines: 3-*tert*-butyl-1-methyl-1*H*-pyrazol-5-yl-amine and 5-*tert*-butyl-1-methyl-1*H*-pyrazol-3-yl-amine were obtained. A mixture of above crude amines (16 mmol, 2.45 g) and 4-chlorophenyl isocyanate (15 mmol, 2.3 g) in DCM (28 mL) was stirred over night at room temperature (see Scheme 1). After removal of solvent *in vacuo*, the crude products (2) and its position

isomer (iso-2) were purified by silica gel chromatography using 50% ethyl acetate in hexane as the eluent.

Rf = 0.15.

^{1}H-NMR (250.13 MHz, DMSO-d$_6$): δ [ppm] = 9.00 (s, 1H, N1H), 8.50 (s, 1H, N2H), 7.50 (d, 2H, aromatic, ^3J = 8.8 Hz), 7.33 (d, 2H, aromatic, ^3J = 8.8 Hz), 6.05 (s, 1H, C4H), 3.60 (s, 3H, CH_3), 1.21 (s, 9H, *tert*-butyl).

^{13}C-NMR (62.9 MHz, DMSO-d$_6$): δ [ppm] = 158.6; 151.8; 138.4; 136.8; 125.6; 31.8 (C), 128.6; 119.7; 94.0 (CH), 34.9; 30.3 (CH_3).

Anal. calcd. for $C_{15}H_{19}ClN_4O$: C 58.73, H 6.24, N 18.26; found: C 58.67, H 6.12, N 18.04.

1-(3-*tert*-Butyl-2-methyl-2*H*-pyrazol-5-yl)-3-(4-chlorophenyl)-urea (iso-2). ^{1}H-NMR (250.13 MHz, DMSO-d$_6$): δ [ppm] = 9.22 (s, br, 1H, N3H), 8.91 (s, 1H, N1H), 7.50 (d, 2H, aromatic, ^3J = 8.8 Hz), 7.32 (d, 2H, aromatic, ^3J = 8.8 Hz), 6.04 (s, 1H, C4H), 3.80 (s, 3H, CH_3), 1.32 (s, 9H, *tert*-butyl).

^{13}C-NMR (62.9 MHz, DMSO-d$_6$): δ [ppm] = 30.9; 93.2; 139.0; 145.3; 151.0; 151.8 (C), 119.7; 128.6; 125.3 (CH), 29.2; 38.6 (CH3).

Anal. calcd. for $C_{15}H_{19}ClN_4O$: C 58.73, H 6.24, N 18.26; found: C 58.66, H 6.21, N 18.35.

1-(5-*tert*-Butyl-2-phenyl-2*H*-pyrazol-3-yl)-3-(4-chlorophenyl)-urea (3). The title compound was prepared according the literature procedure.[7]

^{1}H-NMR (400.13 MHz, $CDCl_3$) δ [ppm] = 7.44 (s, 1H, N1H), 7.23–7.00 (m, 9H, aromatic), 6.79 (s, 1H, N2H), 6.23 (s, 1H, C4H), 1.17 (s, 9H, *tert*-butyl).

^{13}C-NMR (100.6 MHz, $CDCl_3$): δ [ppm] = 162.8; 150.0; 138.0; 136.1; 135.7; 128.0; 32.4 (C), 129.4; 129.1; 127.9; 124.5; 121.5; 97.0 (CH), 30.2 (CH_3).

1-(5-*tert*-Butyl-2-ρ-tolyl-2*H*-pyrazol-3-yl)-3-(4-chlorophenyl)-urea (4). This compound was prepared from the condensation of 5-*tert*-butyl-2-*ρ*-toly-2*H*-pyrazol-3-yl-amine[7] and 4-chlorophenyl isocyanate (see Scheme 1).

A mixture of above amine (7 mmol, 1.5 g) and 4-chlorophenyl isocyanate (7 mmol, 1.07 g) in DCM (14 mL) was stirred over night at room temperature. After removal of solvent *in vacuo* and crystallization from ethyl acetate and hexane (1 : 1) compound (**4**) was isolated as a white powder.

^{1}H-NMR (250.13 MHz, DMSO-d$_6$): δ [ppm] = 9.15 (s, 1H, N3H), 8.37 (s, 1H, N1H), 7.48–7.25 (m, 8H, aromatic), 6.36 (s, 1H, C4H), 2.38 (s, 3H, CH_3), 1.28 (s, 9H, *tert*-butyl).

^{13}C-NMR (62.9 MHz, DMSO-d$_6$): δ [ppm] = 160.5; 151.4; 138.3; 136.9; 136.7; 136.0; 125.5; 31.9 (C), 129.6; 128.6; 124.3; 119.6; 95.1 (CH), 30.1; 20.5 (CH_3).

Anal. calcd. for $C_{21}H_{23}ClN_4O$: C 65.88, H 6.05, N 14.63; found: C 65.62, H 6.09, N 14.87.

MS: *m*/*z* 383.19 (MH^+).

1-(5-*tert*-Butyl-2-σ-tolyl-2*H*-pyrazol-3-yl)-3-(4 chlorophenyl) urea (5). This compound was prepared from the condensation of 5-*tert*-butyl-2-*σ*-toly-2*H*-pyrazol-3-yl-amine[7] and 4-chlorophenyl isocyanate (see Scheme 1).

A mixture of above amine (17 mmol, 3.9 g) and 4-chlorophenyl isocyanate (14.6 mmol, 2.25 g) in DCM (28 mL) was stirred over night at room temperature. After removal of solvent *in vacuo* and crystallization from ethyl acetate and hexane (1 : 1) compound (**5**) was isolated as a white powder.

^{1}H-NMR (250.13 MHz, DMSO-d$_6$): δ [ppm] = 9.08 (s, 1H, N3H), 8.22 (s, 1H, N1H), 7.47–7.30 (m, 8H, aromatic), 6.41 (s, 1H, C4H), 2.04 (s, 3H, CH_3), 1.30 (s, 9H, *tert*-butyl).

^{13}C-NMR (62.9 MHz, DMSO-d$_6$): δ [ppm] = 160.6; 150.9; 138.3; 138.1; 137.0; 136.3; 125.6 32.0 (C), 131.0; 129.1; 128.6; 128.0; 126.7; 119.5; 91.9 (CH), 30.3; 17.0 (CH_3).

Anal. calcd. for $C_{21}H_{23}ClN_4O$: C 65.88, H 6.05, N 14.63; found: C 65.93, H 6.07, N 14.87.

MS: *m*/*z* 383.18 (MH^+).

1-(5-*tert*-Butyl-2-*m*-tolyl-2*H*-pyrazol-3-yl)-3-(4 chlorophenyl) urea (6). This compound was prepared from the condensation of 5-*tert*-butyl-2-*m*-toly-2*H*-pyrazol-3-yl-amine[7] and 4-chlorophenyl isocyanate (see Scheme 1).

A mixture of above amine (7 mmol, 1.5 g) and 4-chlorophenyl isocyanate (7 mmol, 1.07 g) in DCM (14 mL) was stirred over night at room temperature. After removal of solvent *in vacuo* and crystalization from ethyl acetate and hexane (1 : 1) compound (**6**) was isolated as a white powder.

^{1}H-NMR (300 MHz, DMSO-d$_6$): δ [ppm] = 9.6 (s, 1H, N3H), 8.74 (s, 1H, N1H), 7.45–7.13 (m, 8H, aromatic), 6.30 (s, 1H, C4H), 2.30 (s, 3H, CH_3), 1.29 (s, 9H, *tert*-butyl).

^{13}C-NMR (62.9 MHz, DMSO-d$_6$): δ [ppm] = 160.9; 152.1; 139.3; 138.9; 138.4; 137.7; 125.9; 32.4 (C), 129.5; 129.1; 128.5; 125.4; 121.9; 120.0; 96.2 (CH), 30.6; 21.4 (CH_3).

MS: *m*/*z* 383.18 (MH^+).

1-(5-*tert*-Butyl-2-*p*-fluoro-phenyl)-2*H*-pyrazol-3-yl)-3-(4-chlorophenyl)urea (7). This compound was prepared from the condensation of 3-*tert*-butyl-1-(4-fluoro-phenyl)-1*H*-pyrazol-5-amine and 4-chlorophenyl isocyanate (see Scheme 1).

^{1}H-NMR (300 MHz, DMSO-d$_6$): δ [ppm] = 9.12 (s, 1H, N3H), 8.41 (s, 1H, N1H), 7.61–7.31 (m, 8H, aromatic), 6.37 (s, 1H, C4H), 1.22 (s, 9H, *tert*-butyl).

^{13}C-NMR (62.9 MHz, DMSO-d$_6$): δ [ppm] = 163.0; 161.2; 159.7; 152.0; 138.8; 137.6; 1135.4/135.4; 126.1; 32.5 (C), 129.1; 127.1/127.0; 120.1; 116.6/116.3; 96.2 (CH), 30.6 (CH_3).

^{19}F-NMR (372.5 MHz, DMSO-d$_6$): δ [ppm] = −114.6.

MS: *m*/*z* 387.14 (MH^+).

1-(5-*tert*-Butyl-2-*o*-fluoro-phenyl)-2*H*-pyrazol-3-yl)-3-(4-chlorophenyl)urea (8). This compound was prepared from the condensation of 5-*tert*-butyl-2-(2-fluoro-phenyl)-2*H*-pyrazol-3-yl-amine and 4-chlorophenyl isocyanate (see Scheme 1).

^{1}H-NMR (300 MHz, DMSO-d$_6$): δ [ppm] = 9.06 (s, 1H, N3H), 8.45 (s, 1H, N1H), 7.71–7.31 (m, 8H, aromatic), 6.42 (s, 1H, C4H), 1.23 (s, 9H, *tert*-butyl).

^{13}C-NMR (62.9 MHz, DMSO-d$_6$): δ [ppm] = 158.6; 155.3; 131.2/131.3; 126.3/126.2; 126.1; 125.7/125.6; 117.4/117.1; 32.5 (C), 162.0; 151.4; 139.1/138.6; 130.1; 129.1; 120.0; 93.6 (CH), 30.8 (CH_3).

^{19}F-NMR (372.5 MHz, DMSO-d$_6$): δ [ppm] = −121.3.

MS: *m*/*z* 387.14 (MH^+).

1-(5-*tert*-Butyl-2-*p*-methoxy-phenyl)-2*H*-pyrazol-3-yl)-3-(4-chlorophenyl)urea (9). This compound was prepared from the condensation of 3-*tert*-butyl-1-(4-methoxyphenyl)-1*H*-

pyrazol-5-amine and 4-chlorophenyl isocyanate (see Scheme 1).

^{1}H-NMR (300 MHz, DMSO-d_6): δ [ppm] = 9.15 (s, 1H, N3H), 8.34 (s, 1H, N1H), 7.47–7.07 (m, 8H, aromatic), 6.36 (s, 1H, C4H), 3.83 (s, 3H, OCH_3), 1.29 (s, 9H, *tert*-butyl).

^{13}C-NMR (62.9 MHz, DMSO-d_6): δ [ppm] = 160.7 ; 158.9; 151.8; 138.9; 137.5; 131.8; 126.0; 32.4 (C), 127.1; 126.4; 119.6; 114.8; 94.9 (CH), 55.9; 30.7 (CH_3).

MS: *m*/*z* 399.16 (MH^+).

1-(5-*tert*-Butyl-2-*o*-methoxy-phenyl)-2*H*-pyrazol-3-yl)-3-(4-chlorophenyl)urea (10). This compound was prepared from the condensation of 3-*tert*-butyl-1-(2-methoxyphenyl)-1*H*-pyrazol-5-amine and 4-chlorophenyl isocyanate (see Scheme 1).

^{1}H-NMR (300 MHz, DMSO-d_6): δ [ppm] = 9.21 (s, 1H, N3H), 8.16 (s, 1H, N1H), 7.55–7.14 (m, 8H, aromatic), 6.36 (s, 1H, C4H), 3.81 (s, 3H, OCH_3), 1.27 (s, 9H, *tert*-butyl).

^{13}C-NMR (62.9 MHz, DMSO-d_6): δ [ppm] = 161.1 ; 154.3; 151.1; 139.0; 138.8; 130.6; 126.0; 32.5 (C), 129.7; 129.1; 127.0121.2; 119.9; 113.3; 92.1 (CH), 56.2; 30.7 (CH_3).

MS: *m*/*z* 399.16 (MH^+).

1-(5-*tert*-Butyl-2-*p*-chloro-phenyl)-2*H*-pyrazol-3-yl)-3-(4-chlorophenyl)urea (11). This compound was prepared from the condensation of 3-*tert*-butyl-1-(2-chloro-phenyl)-1*H*-pyrazol-5-amine and 4-chlorophenyl isocyanate (see Scheme 1).

^{1}H-NMR (300 MHz, DMSO-d_6): δ [ppm] = 9.13 (s, 1H, N3H), 8.46 (s, 1H, N1H), 7.66 (s, 4H, aromatic), 7.44 (dd, 4H, aromatic), 6.38 (s, 1H, C4H), 1.29 (s, 9H, *tert*-butyl).

^{13}C-NMR (62.9 MHz, DMSO-d_6): δ [ppm] = 161.6 ; 152.1; 138.8; 137.9; 137.6; 131.9; 32.5 (C), 129.6; 129.1; 126.1; 120.1; 96.9 (CH), 30.5 (CH_3).

MS: *m*/*z* 403.13 (MH^+).

1-(5-*tert*-Butyl-2-*o*-chloro-phenyl)-2*H*-pyrazol-3-yl)-3-(4-chlorophenyl)urea (12). This compound was prepared from the condensation of 3-*tert*-butyl-1-(2-chloro-phenyl)-1*H*-pyrazol-5-amine and 4-chlorophenyl isocyanate (see Scheme 1).

^{1}H-NMR (300 MHz, DMSO-d_6): δ [ppm] = 8.99 (s, 1H, N3H), 8.32 (s, 1H, N1H), 7.74–7.30 (m, 8H, aromatic), 6.40 (s, 1H, C4H), 1.28 (s, 9H, *tert*-butyl).

^{13}C-NMR (62.9 MHz, DMSO-d_6): δ [ppm] = 161.7 ; 151.2; 139.1; 138.6; 136.0; 126.1; 32.5 (C), 132.3; 131.4; 131.1; 130.7; 129.1; 128.3; 120.0; 92.5 (CH), 30.6 (CH_3).

MS: *m*/*z* 403.13 (MH^+).

Crystal structure determinations. Crystallographic data of compounds (2), (3), (4), (5) and (6) have been deposited with Cambridge Crystallographic Data Center.

Biophysical investigation

Protein production

Murine p38α kinase (2–349) was cloned, expressed and purified as described in our previous work.[11]

For expression of phosphorylated active p38α kinase, the S599D/T603D MKK6/SKK3 activated mutant was co-expressed with p38α kinase. This activation mutant of MKK6/SKK3 is needed, since its expression in *E. coli* results in an inactive state. For co-expression, both kinase genes were cloned into the pETDuet (Novagen, Madison, WI, USA) vector, which is designed for the co-expression of two target genes.

Instrumentation

The MST measurements were performed on a Nanotemper Monolith NT.115 instrument. A MST power of 40% and a LED power of 50% with a laser on time of 30 seconds and a laser off time of 5 seconds were used. Analysis was performed with NanoTemper Analysis Software and calculated IC50 competition values were converted to K_i values using the K_i http://sw16.im.med.umich.edu/software/calc_ki/) analysis was performed with NanoTemper Analysis Software.

Microscale thermophoresis (MST)

Competition assay. All compounds were diluted into a buffer containing 50 mM Tris pH 7,6, 150 mM NaCl, 10 mM $MgCl_2$ and 0.05% Tween20. The final DMSO concentration was adjusted to 5% (v/v) in the dilution series. A premix containing 80 nM (or 160 nM) p38α kinase and 25 nM Kinase tracer 199 (Life Technologies) was prepared. 10 μl of each compound concentration was mixed with 10 μl of the premix containing kinase tracer 199 and p38α kinase.

Acknowledgements

H. S. is member of the DFG-funded cluster of excellence: macromolecular complexes. K. S. is supported by SFB807. The work present here has been conducted within the center for translational cancer research, DKTK. BMRZ is supported by the state of Hesse. The authors would like to thank Dr. Gerd Nielsen for her support in running the NMR experiments.

Notes and references

1 J. C. Lee, J. T. Laydon, P. C. McDonnell, T. F. Gallagher, S. Kumar, D. Green, D. McNulty, M. J. Blumenthal, J. R. Heys, S. W. Landvatter, J. E. Strickler, M. M. McLaughlin, I. R. Siemens, S. M. Fisher, G. P. Livi, J. R. White, J. L. Adams and P. R. Young, *Nature*, 1994, **372**, 739.
2 P. Cohen, *Nat. Rev. Drug Discovery*, 2002, **1**, 309.
3 J. Dumas, *Curr. Opin. Drug Discovery Dev.*, 2002, **5**, 718.
4 G. Manning, D. B. Whyte, R. Martinez, T. Hunter and S. Sudarsanam, *Science*, 2002, **1912**, 298.
5 R. Roskoski Jr., *Pharmacol. Res.*, 2016, **103**, 26.
6 C. Pargellis, L. Tong, L. Churchill, P. F. Cirillo, T. Gilmore, A. G. Graham, P. M. Grob, E. R. Hickey, N. Moss, S. Pav and J. Regan, *Nat. Struct. Biol.*, 2002, **9**, 268.
7 J. Regan, S. Breitfelder, P. F. Cirillo, T. Gilmore, A. G. Graham, E. R. Hickey, B. Klaus, J. Madwed, M. Moriak, N. Moos, C. Pargellis, S. Pav, A. Proto, A. Swinamer, L. Tong and C. Torcellini, *J. Med. Chem.*, 2002, **45**, 2994.
8 Z. Zhao, H. Wu, L. Wang, Y. Liu, S. Knapp, Q. Liu and N. S. Gray, *ACS Chem. Biol.*, 2014, **6**, 1230.
9 J. Regan, A. Capolino, P. F. Cirillo, T. Gilmore, A. G. Graham, E. R. Hickey, R. R. Kroe, J. Madwed, M. Moriak, R.

Nelson, C. A. Pargellis, A. Swinamer, C. Torcellini, M. Tsang and N. Moos, *J. Med. Chem.*, 2003, **46**, 4676.

10 (*a*) N. Moss, S. Breitfelder, R. Betageri, P. F. Cirillo, T. Fadra, E. R. Hickey, T. Kirrane, R. R. Kroe, J. Madwed, R. M. Nelson, C. A. Pargellis, K. C. Qian, J. Regan, A. Swinamer and C. Torcellini, *Bioorg. Med. Chem.*, 2003, **13**, 3101; (*b*) S. T. Onions, K. Ito, C. E. Charron, R. J. Brown, M. Colucci, F. Frickel, G. Hardy, K. Joly, J. King-Underwood, Y. Kizawa, I. Knowles, P. J. Murray, A. Novak, A. Rani, G. Rapeport, A. Smith, P. Strong, D. M. Taddei and J. G. Williams, *J. Med. Chem.*, 2016, **5**, 1727.

11 (*a*) J. Regan, C. A. Pargellis, P. F. Cirillo, T. Gilmore, E. R. Hickey, G. W. Peet, A. Proto, A. Swinamer and N. Moss, *Bioorg. Med. Chem.*, 2003, **13**, 3101; (*b*) T. Arai, M. Ohno, H. Inoue, S. Hayashi, T. Aoki, H. Hirokawa, H. Meguro, Y. Koga, K. Oshida, M. Kainoh, K. Suyama and H. Kawai, *Bioorg. Med. Chem.*, 2012, **15**, 5118.

12 J. R. Simard, M. Getlik, C. Grütter, V. Pawar, S. Wulfert, M. Rabiller and D. Rauh, *J. Am. Chem. Soc.*, 2009, **37**, 13286.

13 M. Vogtherr, K. Saxena, S. Hoelder, S. Grimme, M. Betz, U. Schieborr, B. Pescatore, M. Robin, L. Delarbre, T. Langer, K. U. Wendt and H. Schwalbe, *Angew Chem., Int. Ed.*, 2006, **45**, 993.

14 P. Linke, K. Amaning, M. Maschberger, F. Vallee, V. Steier, P. Baaske, S. Duhr, D. Breitsprecher and A. Rak, *J. Biomol. Screening*, 2015, 1–8.

15 M. Jerabek-Willemsena, T. Andréa, R. Wannera, H. Marie Rotha, S. Duhra, P. Baaskea and D. Breitsprechera, *J. Mol. Struct.*, 2014, **1077**, 101.

16 G. J. Zaman, M. M. van der Lee, J. J. Kok, R. L. Nelissen and E. E. Loomans, *Assay Drug Dev. Technol.*, 2006, **4**, 411.

17 G. Nielsen and H. Schwalbe, *ChemBioChem*, 2011, **17**, 2599.

18 A. Kuglstatter, M. Ghate, S. Tsing, A. G. Villaseñor, D. Shaw, J. W. Barnett and M. F. Browner, *Bioorg. Med. Chem. Lett.*, 2010, **17**, 5217.

19 H. Lavoie, N. Thevakumaran, G. Gavory, J. J. Li, A. Padeganeh, S. Guiral, J. Duchaine, D. Y. Mao, M. Bouvier, F. Sicheri and M. Therrien, *Nat. Chem. Biol.*, 2013, **7**, 428.

20 S. Han, A. Mistry, J. S. Chang, D. Cunningham, M. Griffor, P. C. Bonnette, H. Wang, B. A. Chrunyk, G. E. Aspnes, D. P. Walker, A. D. Brosius and L. Buckbinder, *J. Biolumin. Chemilumin.*, 2009, **19**, 13193.

21 J. Dong, H. Zhao, T. Zhou, D. Spiliotopoulos, C. Rajendran, X. D. Li, D. Huang and A. Caflisch, *ACS Med. Chem. Lett.*, 2014, **1**, 79.

22 W. L. Delano, *The PyMOL Molecular Graphics System*, 2002.

23 (*a*) B. F. Thomas, Y. Zhang, M. Brackeen, K. M. Page, S. W. Mascarella and H. H. Seltzman, *AAPS J.*, 2006, **8**, E665; (*b*) *The cannabinoid receptors*, ed. P. Reggio, 2009, p. 95.

24 K. Ikegashira, T. Oka, S. Hirashima, S. Noji, H. Yamanaka, Y. Hara, T. Adachi, J. Tsuruha, S. Doi, Y. Hase, T. Noguchi, I. Ando, N. Ogura, S. Ikeda and H. Hashimoto, *J. Med. Chem.*, 2006, **49**, 6950.

